ELSEVIER

Int. J. Therm. Sci. 41 (2002) 173–181

International Journal of Thermal Sciences

Electro-thermal simulation of an ultra stable quartz oscillator ☆

Serge Galliou *, Marc Mourey

Laboratoire de Chronométrie Électronique et Piézoélectricité, École Nationale Supérieure de Mécanique et des Microtechniques, 26, Chemin de l'Épitaphe, 25000 Besançon, France

Received 9 October 2000; accepted 7 March 2001

Abstract

Ultra Stable quartz Oscillators (USO) which can exhibit relative frequency fluctuations of a few 10^{-10} when the ambient temperature ranges from 243 K (−30 °C) to 343 K (+70 °C) should all be ovenized to achieve ultimate performance. Such a result needs a very large static thermal gain close to 1000 in the vicinity of the quartz resonator case. Basically, the problem consists in regulating a volume with distributed thermal losses at its edge and internal heat sources whereas just the temperature at one point, the sensor temperature, is known.

So, the feedback control system simulation involves a mixture of thermal and electronic functions. To solve this problem we use the electrical analogy for the thermal part. The thermal mesh is still manually done but a unique computer aided software dedicated to electronic circuit simulation will efficiently provide a solution.

This choice is discussed and the example of an USO thermal regulator is described as an illustration of this methodology.

Keywords: Temperature regulator; Oven control; Electro-thermal simulation; Quartz oscillator

1. Introduction

Ultra Stable quartz Oscillator (USO) are commonly used in navigation and positioning systems of ships, aircrafts or satellites. In this field, the best oscillators exhibit relative frequency fluctuations of a few 10^{-10} when the ambient temperature ranges from 243 K (−30 °C) to 343 K (+70 °C) and a relative frequency stability better than 1 10^{-13} can be achieved for measuring times between 1 second and 100 seconds [1]. These results can be obtained only if the internal structure of the USO is precisely ovenized (then we speak about oven-controlled crystal oscillators OCXO). The most temperature-sensitive element of the USO is its heart, namely the quartz resonator, but in fact the influence of ambient temperature changes must be reduced on the main part of the electronics. Roughly this means that the temperature change at the level of the resonator case should not fluctuate more than a few 10^{-1} K in steady state when the ambient temperature change is 100 K whereas a few degrees of temperature change is acceptable for the remaining volume (about 250×10^{-6} m^3).

Other constraints often exist such as a limited power consumption during the warm-up time and/or in steady state, a specific supply voltage … Moreover, for space applications the oscillator must be able to work under vacuum—in space—as well as into the air—on earth—which means two different boundary conditions for the thermal problem and moreover it must withstand vibrations and accelerations during the launch which also means interactions between thermal and mechanical designs.

So, in other words the oscillator design involves the thermal regulation of a volume from the knowledge of the temperature at one point of this volume (usually one point but sometimes two points or more) by monitoring local heat fluxes while considering that internal heat sources exist. As a consequence the feedback control system simulation includes a mixture of thermal and electronic functions.

The methodology that we are using to simulate this problem is described below.

☆ This work is mainly supported by the Centre National d'Etudes Spatiales (CNES), the French space agency.

* Correspondance and reprints.

E-mail addresses: serge.galliou@ens2m.fr (S. Galliou), marc.mourey@ens2m.fr (M. Mourey).

1290-0729/02/$ – see front matter
PII: S1290-0729(01)01295-9

Nomenclature

a	first order coefficient of the static frequency-temperature relationship	K^{-1}
$\tilde{a}$	dynamic frequency-temperature coefficient	$s{\cdot}K^{-1}$
e	plate width	m
f_0	oscillator frequency	Hz
f_Q	the resonant frequency of the quartz resonator	Hz
h	convection exchange coefficient	$W{\cdot}K^{-1}{\cdot}m^{-2}$
$I, I_{nm}, i(V_{msond})\ldots$	electric currents equivalent to thermal fluxes in the electrical analogy	A
l	plate length	m
$R[T], R[v(in)\ldots]$	thermal or equivalent electrical resistors	$K{\cdot}W^{-1}$ or Ω
S	surface	m^2
$T, T_0, T_e, T_{amb}\ldots$	temperatures	K
T_Q	the mean temperature of the quartz resonator	K
$V(n), V(m)\ldots$	electric voltages equivalent to temperatures in the electrical analogy	V
Δf	frequency change	Hz
$\Delta T, \Delta T_e, \Delta T_{moy}\ldots$	temperature changes	K

Greek symbols

α	dimensionless factor	
φ	thermal flux per unit area	$W{\cdot}m^{-2}$
λ	thermal conductivity	$W{\cdot}K^{-1}{\cdot}m^{-1}$
σ	Stefan constant $= 5.670 \times 10^{-8}$	$W{\cdot}m^{-2}{\cdot}K^{-4}$

2. Some figures

Fig. 1 shows a basic sketch of a quartz oscillator. In fact the oscillator output frequency f_o is not exactly equal to the resonant frequency f_Q of the quartz crystal resonator but is slightly shifted from it (typically a few Hertz at 10 MHz) by the amplifier electronics. So, any external physical quantity like temperature that could modify the electronic behaviour as well as the resonator behaviour should disturb the oscillator output frequency stability.

The thermal sensitivity of the loop amplifier can be evaluated as $(\Delta f/f)/\Delta T \approx 10^{-10}$ K^{-1}. Nevertheless the most temperature sensitive element of a quartz oscillator is its resonator which exhibits a relative frequency deviation $\Delta f_Q/f_Q$ greater than 2×10^{-5} when its temperature T_Q moves from 243 K (−30 °C) to 343 K (+70 °C). In steady-state conditions the quartz resonant frequency f_Q is related to its temperature T_Q according to a third order polynomial function. Otherwise an additional term $\tilde{a}\,dT_Q/dt$ must be considered to take into account the dynamic temperature sensitivity [2,3].

Of course it is convenient to set the operating temperature of the thermal regulator to one of both resonator turn-over temperatures if possible. Usually the cut angles of the crystal are adjusted in order to get it close to 353 K (80 °C). Thus, in the usual external temperature range this desired temperature can be sustained into the oscillator enclosure by just heating (cooling is not needed). In fact it is impossible to lock indefinitely the operating point at the optimum point of the frequency-temperature curve: drift always exists due to component ageing for example and must be taken into account. So, at an operating temperature distant of 0.5 K (see Fig. 1) from the turn-over temperature of the resonator (an equivalent temperature drift of 0.5 K is a realistic data for a ten years old oscillator!) the relative resonant frequency deviation versus temperature can be simply expressed as $\Delta f_Q/f_Q \approx a\Delta T_Q + \tilde{a}\,dT_Q/dt$ where $a \approx 2.510^{-9}$ K^{-1} and

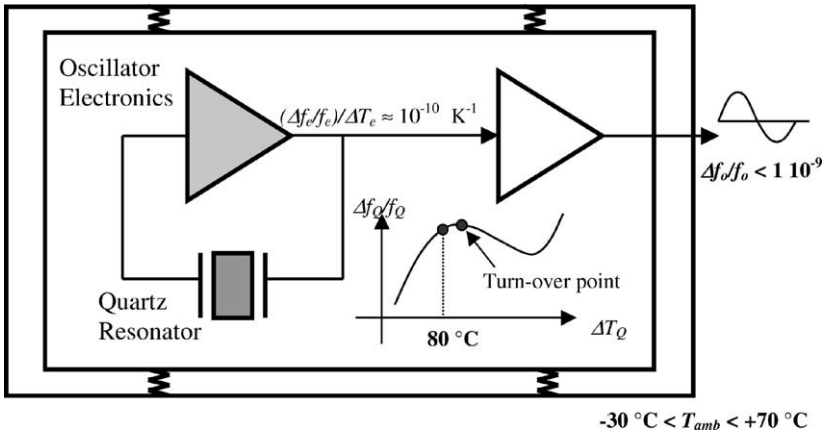

Fig. 1. A quartz oscillator is basically a closed-loop system including the quartz resonator an its amplifier. Both elements are temperature sensitive. The relative frequency change of the resonator is typically $\Delta f_Q/f_Q > 2 \times 10^{-5}$ when its temperature T_Q is between −30 °C and +70 °C.
So, it is obvious that a thermal processing is necessary in order to reach $\Delta f_o/f_o < 1 \times 10^{-9}$ at the oscillator output.

$\tilde{a} \approx 2 \times 10^{-7}$ s·K^{-1} for the crystal cuts in which we are interested.

Previous figures point out the importance of the dynamic behaviour of the resonator. Fortunately for a BVA resonator type [4] the assembly of the crystal in its case performs a thermal filtering effect, acting like a kind of second order low-pass filter which exhibit a low cut-off frequency of a few tenths of millihertz (in a few words, the BVA structure—BVA for "Boîtier à Vieillissement Amélioré" in French—is an electrodeless quartz resonator clamped between a couple of quartz lenses which are one-face metallized. This "sandwich" is sustained by springs into a metallic cylinder inside its case under vacuum. Gold is not laid down directly onto the resonator surfaces so ageing is improved).

Finally a "natural filtering" of fast thermal fluctuations is effective in the case of a BVA resonator structure due to its thermal inertia. This low-pass filtering is added to the one of the overall oscillator insulation and enclosure. Thus, the main design problem remains the thermal regulator in order to cancel slow thermal drifts.

Furthermore it is interesting to keep in mind that the overall thermal insulation can achieve a maximum value of 20 K·W^{-1} (it is difficult to get better with a 500×10^{-6} m^3 oscillator) and that the inner power consumption of the electronics, with the thermal regulation off, is usually about 1 Watt. This could lead to a temperature offset up to 20 K: this means that the maximum external temperature would be limited to 333 K with an internal operating temperature set at 353 K! (on the other hand greater the insulation is, lower the overall power consumption will be) .... Note that the use of insulation foam are often prohibited in space applications.

3. Our choice of simulation tool

Simple evaluations must be completed to take into account the fact that thermal losses and fluxes are distributed and that they are non-homogeneous. Just a limited number of typical thermal problems can be analytically solved.

Let us consider an enclosure surrounding our resonator case (or the oscillator electronics) having a temperature locally set to T_0. Its behaviour may be partly described by a conductive plate fin (see Fig. 2) having width e along the y axis, whose temperature is $T(x, y)$. Its temperature is constant, equal to T_0 at $x = 0$, and it is adiabatic at the other end $x = l$ (this may be a symmetry condition for a half-enclosure) as well as across its plane $y = 0$, while the heat flux per unit area is $\varphi = h(T - T_e)$ across its insulated face (T_e is the external temperature).

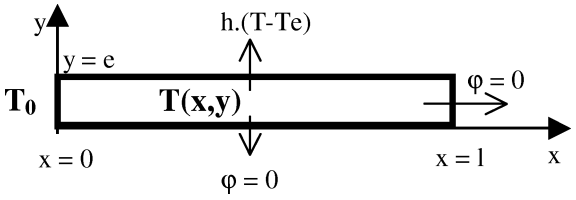

Fig. 2. A basic model for a thermal analysis.

In our application the longitudinal heat flux which is flowing across a metallic material, is much greater than the lateral one. Hence the temperature distribution is almost independent of y, that is:

$$T^*(x, y) \approx T^*(x) = \frac{T - T_e}{T_0 - T_e} = \frac{ch[m(l - x)]}{ch[ml]} \tag{1}$$

where $m^2 = h/\lambda e$, λ being the plate thermal conductivity. The mean temperature of *T(x)* along the plate can then be expressed as (2):

$$T_{mean} = \frac{1}{l} \int_{x=0}^{x=l} T(x)\,dx = T_e + (T_0 - T_e)\frac{th[ml]}{ml} \tag{2}$$

A criterion of thermal regulation quality could be the following gain given by (3), where ΔT_{mean} is the change of the mean temperature T_{mean} for an external temperature change ΔT_e.

$$G = \frac{\Delta T_e}{\Delta T_{mean}} = \left(1 - \frac{th[ml]}{ml}\right)^{-1} \tag{3}$$

Applying this relationship (3) with the dimensions and materials usually used in USO we never get G better than 300 whereas we need 1000 at least! Several solutions exist:

- One of them consists in adding an extra thermal regulated enclosure. This solution leads to very good results once the adjustments were done but these ones are quite difficult. The reference temperature of the added enclosure surrounding the previous one must be tuned indeed between the operating point of the latter and the maximum external temperature. It is set by taking into account the inner power to be dissipated and according to the thermal links (or insulation) between both enclosures on the one hand and with the external case on the other hand. Finally, the feedback parameters must be tuned in order to avoid couplings of both regulators that easily occurred. In the case of an USO intended for space applications the thermal regulation problem is complicated: this USO must be temperature controlled in the air as well as under vacuum and must be vibration-proof, which involves a reinforced structure and various thermal boundary conditions.
- A second one consists of sharing out the processed power. Thus the power part which is taken away from the temperature sensor—that is, which is set on the thermal path from the sensor to the ambient temperature—has the same effect than an increasing of the insulation resistor and as a consequence of the thermal gain. The main difficulty is still there the feedback adjustment once the optimum heater position was found.
- A third solution is based on a compensation effect provided that the temperature disturbance is detected. This needs to send back a second temperature sensor

information to the regulation monitoring. Compensation is equivalent to a small reference temperature change that is a slight positive feedback.

Thus, as already mentioned above, in any case the sensor and power element positions involves matching of the regulator electronics, first to avoid instabilities and second to improve the thermal regulation efficiency. Anyway feedback adjustments are needed.

The analytical calculus is difficult to apply to complex structures made of an assembly of various elements. The numerical simulation of the thermal problem often becomes the only possible alternative: this is the interest of a computer program based on finite element or finite difference methods. Nevertheless they are able to solve the purely thermal aspect but cannot process easily the control of a temperature by monitoring the applied power (every time in transient analysis) in order to lock the sensor temperature at the reference value whatever the ambient temperature fluctuations are.

The electronic functions of the temperature regulation are as essential as the thermal ones. They can be simulated accurately with a CAD program dedicated to electronic circuits.

Consequently the overall temperature control simulation would then need an interface between the finite element software and the electronic simulation one, the data exchanges between both being made at every calculation step. This solution is not unrealisable but perhaps a little heavy.

The remarks above led us to process the whole problem by only one software while bringing back the thermal part as an electrical network by analogy. Thus using this classical thermal nodal method, volumes are discretized and identified to a set of capacitors, associated to six resistors per node [5–8]. Boundary conditions also leads to link resistors or current generators (temperatures becomes voltages and heat fluxes are equivalent to electrical currents). Once the analogy is performed (presently this is manually done: here is the main limitation of the method), the electrical equivalent network can be directly associated with the functional or behavioural models of the electronic components used for the regulation loop.

Thus, feedback elements can easily be adjusted and fruitful simulation results can be extracted: they could be thermal data such a maximum local temperature in the structure as well as the maximum current through a specified component in order to applied derating requirements applicable to electronics for instance.

4. An example

Fig. 3 illustrates a simplified mesh of an USO structure (more exactly 1/8 of the structure because of the symmetries) including an oven in which the resonator is adjusted. This oven is fixed between two printed circuit boards positioned into a μ-metal enclosure. The latter is hung on the external case (not represented in Fig. 3) by means of special supports. To illustrate the electrical analogy actually applied, one sub-part (concerning the internal case) of the corresponding global equivalent electrical network is shown in Fig. 4: it is obvious that interesting areas could be meshed more accurately. In Fig. 4 for example, the conductive exchange between the inner case and the external case across the support are just modelled by the resistor "*Rsupport*". Radiative exchanges under vacuum (or by conduction plus convection into the air) are also simply modelled by resistor. They could be generalised with voltage-controlled current sources which look like $I_{nm} = \alpha \cdot S \cdot \sigma \cdot [V^4(n) - V^4(m)]$, n and m denoting nodes of both exchanging surfaces, S being the element surface and α a factor depending on the emissivities of both surfaces and related to their view factor [5]. In the same way, conduction or/and convection could be described by a relationship such $I = h \cdot S \cdot [V(n) - V(m)]$. One can also notice that the dissipated power of electronic components can be taken into account (see the current source *IDC* in Fig. 4). Ports such those called "*probe1*" and "*ovenpower*" allow to link one layer modelling the thermal structure (Fig. 4) to a second one modelling the electronic functions. In a first stage this last one is just limited to the functional model of a simple regulator as shown in Fig. 5. In this example the total monitored power is simply equal to 1000 times the error signal—the difference between the feedback signal from the sensor "*probe1*" and the reference temperature set to 353 K (80 °C)—up to a maximum

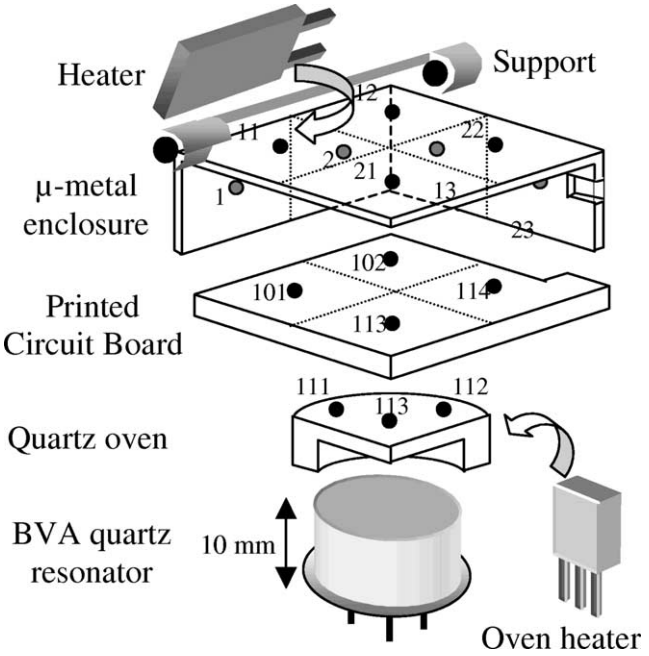

Fig. 3. A simplified mesh of 1/8 of the structure. The external enclosure is not represented. Each node will be attached to a capacitor and six resistors in the electrical analogy of the thermal problem. In the actual device the electronic components (of the oscillator loop, the intermediate stage and the output amplifier, the voltage supplies, the temperature regulator) are positioned on the PCBoards and also on the outer surface of the μ-metal enclosure.

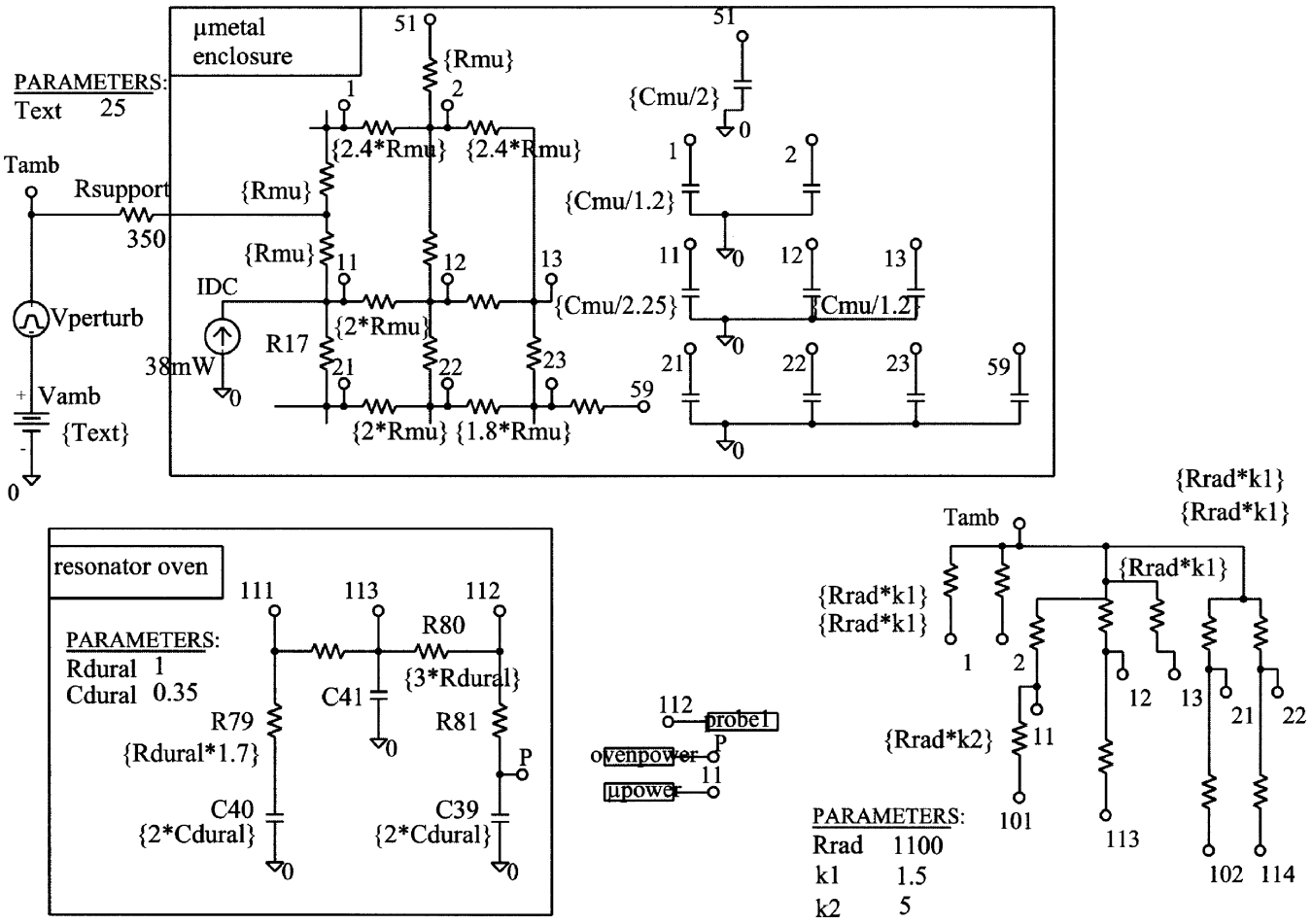

Fig. 4. A sub-part of the equivalent electrical network for the thermal analysis of the structure shown in Fig. 3. "*probe1*" (corresponding to the thermistor) "*ovenpower*" (corresponding to the oven heater of Fig. 3) and "μ *power*" (corresponding to the μ-metal heater of Fig. 3) are links with the electronic part of the thermal regulator (see Fig. 5 or Fig. 6). In this example, when the oscillator operates under vacuum, the non-linear behaviour of radiative exchanges can be neglected. Thus, one can write $I_{nm} = \alpha \cdot S \cdot \sigma \cdot [V^4(n) - V^4(m)] \approx \alpha \cdot (Rrad)^{-1} \cdot [V(n) - V(m)]$. This is why radiative exchanges between elemental surfaces are modelled as resistors $k_i \,.\, Rrad$ where $k_i = \alpha^{-1}$ with $\varepsilon_n \cdot \varepsilon_m < \alpha < \varepsilon_n \cdot \varepsilon_m / [1 - (1 - \varepsilon_n) \cdot (1 - \varepsilon_m)]$, ε_n and ε_m being the emissivity of both surfaces (the default values of k_i are indicated here). The model $k_i \,.\, Rrad$ is still used when convection and conduction become predominant for operation in the air, provided that k_i is adjusted.

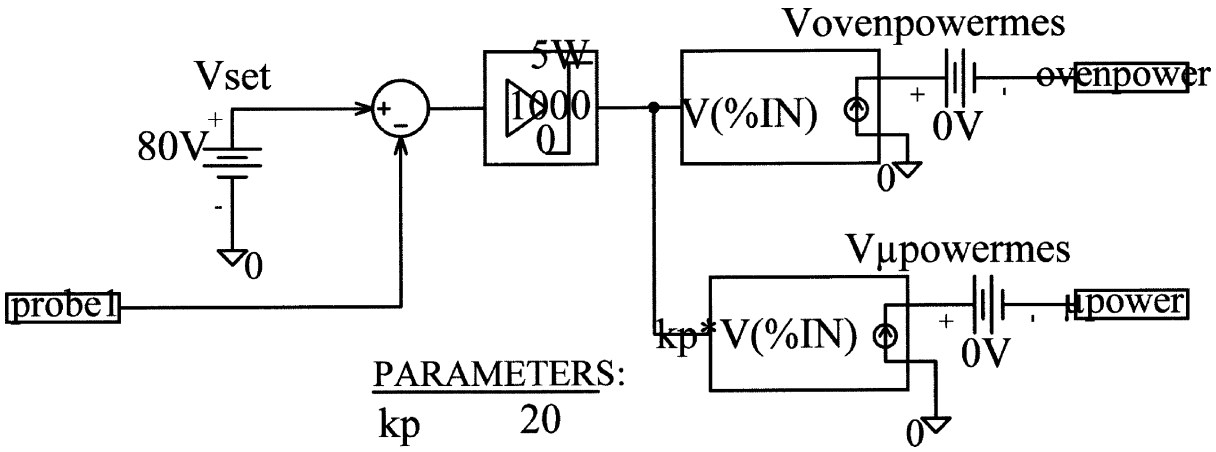

Fig. 5. A functional model of the electronic part. This is the simplest way to implement the feedback loop of the thermal regulator. One can recognize some basic functions such as an error detector, a proportional amplifier (gain 1000) limited from 0 to 5 W, an two actuators which are just here voltage-controlled sources. The parameter k_p, here with a default value of 20, is the adjustable power ratio between the monitored power applied on the oven and its part applied on the μ-metal can.

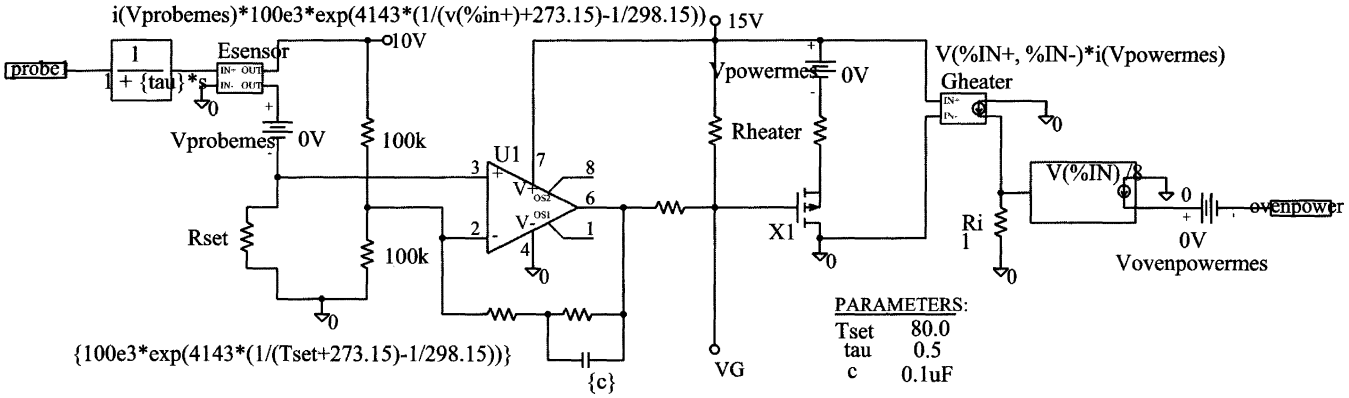

Fig. 6. The heart of the electronic part of the thermal regulation. This is one way to perform the upper part of the functional model of Fig. 5. Here X1 could be the "oven heater" in Fig. 3. VG is the monitoring voltage of other power sources ("μ *power*" in Fig. 4). Note the "temperature"-to-resistor input conversion and the electrical power-to-thermal flux output conversion.

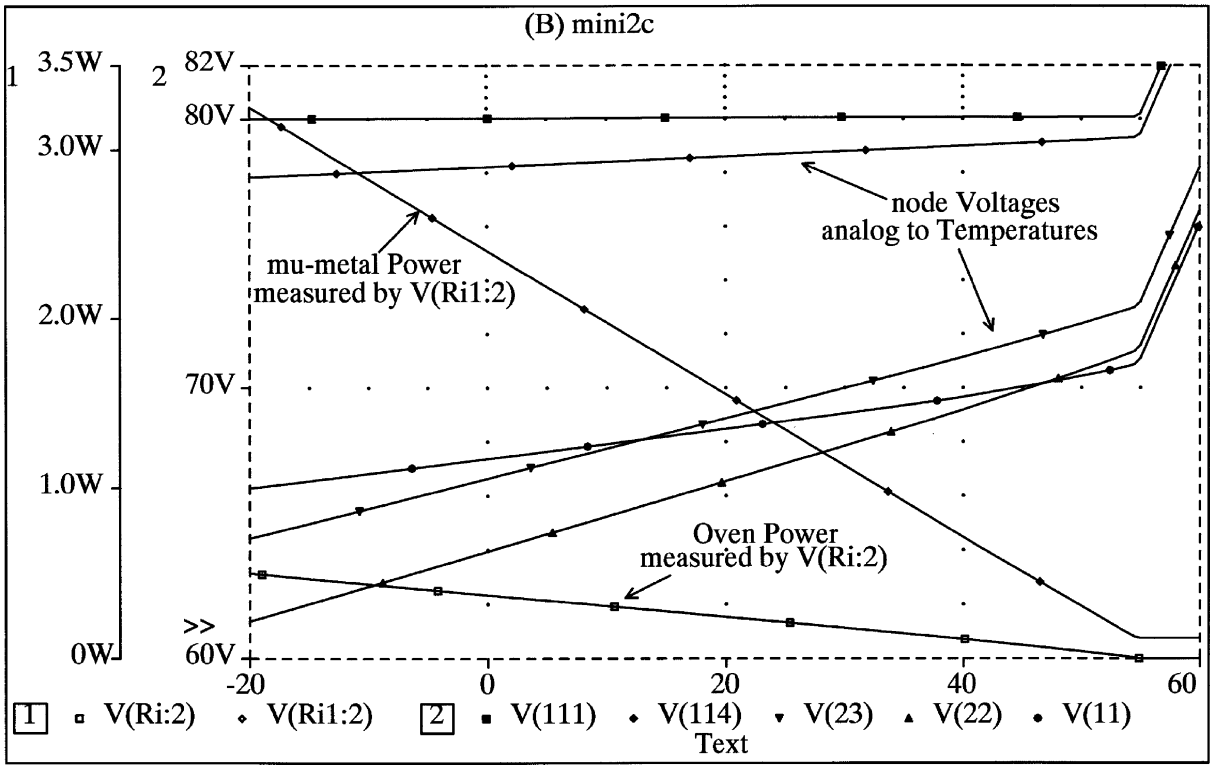

Fig. 7. Graphical output of the electronic circuit simulator SPICE after a DC analysis, i.e., in steady state (Volts are equivalent to Celsius degrees in the electrical analogy). The *Y* axis #1 (from 0 W to 3.5 W) gives scales of monitored powers versus the external temperature *Text* (the node T_{amb} in Fig. 4 has the value *Text* from -20 to $+60$). Here the thermal regulator turns off when the ambient temperature reaches a little bit more than 50 °C (323 K). The *Y* axis #2 (increasing from 60 V to 82 V, i.e., from 60 °C = 333 K to 82 °C = 355 K) gives scales of some node voltages (i.e., temperatures). As an illustration of the regulator efficiency the node #111 (see Fig. 4) close to the thermistor location (node #112 in Fig. 4) does not move significantly because it is locked at the reference temperature (80 V or °C) whereas the node #22 is more sensitive to *Text*. A zoom on the node #111 trace would exhibit a static gain of about 1000.

value here limited to 5 Watts. This first simulation gives the orders of magnitude of the temperature changes, and loop adjustments can be carried out in static and dynamic conditions. In a second stage the system performances can eventually be improved using multiple regulation and/or distribution of powers and/or compensation (in Fig. 5 the monitored power is shared in one part ("*ovenpower*") close to the sensor ("*probe1*") and an other part more far from it ("μ *power*").

The second stage is probably the most important one. It consists in converting the previous functional model in a more realistic way. Thereby the upper part of Fig. 5 could be implemented as in Fig. 6. Let us focus our attention on the input and output of this electronic module.

At the input of the electronic function of the thermal regulator there is the thermal sensor equivalent to a temperature converter into an electrical quantity. Here the temperature sensor is a thermistor modelled by a voltage-controlled

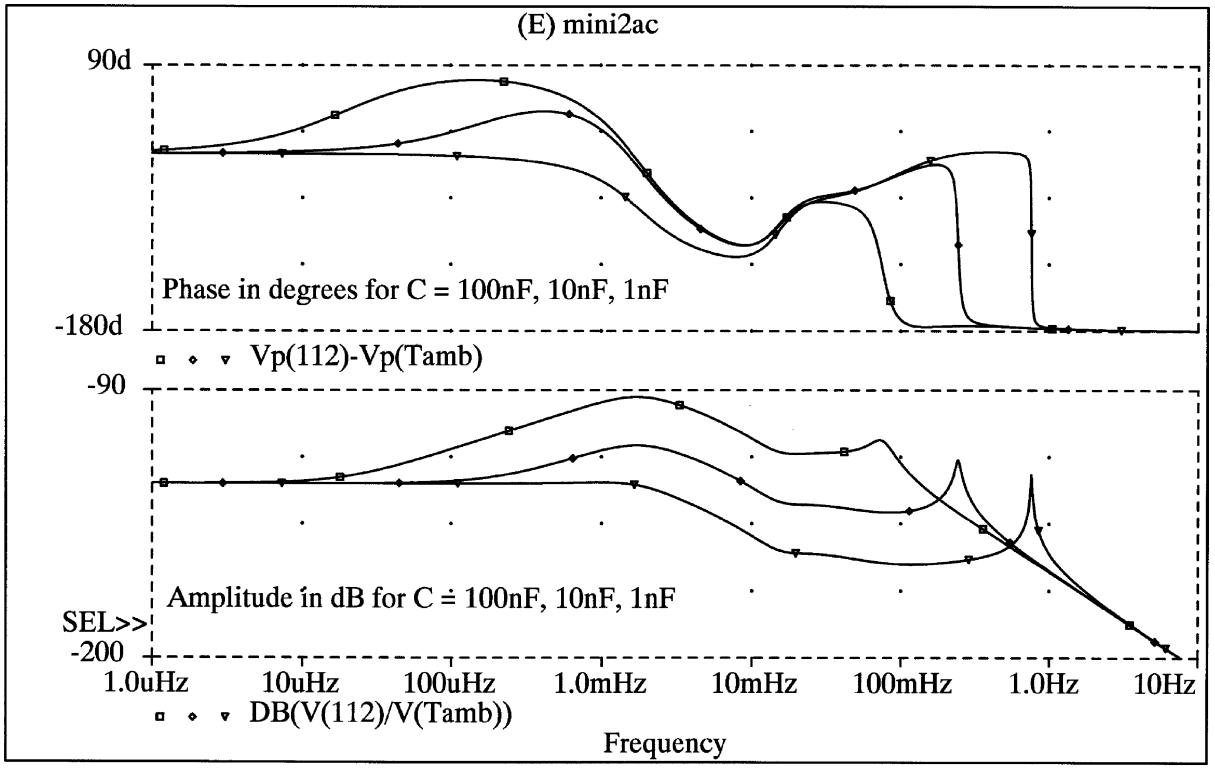

Fig. 8. AC analysis at node #112 (i.e., frequency response) when the ambient temperature *Tamb* is disturbed according to a sine way with a frequency swept from 1 μ Hz to 10 Hz (see the X axis variable), for three different values of *c* (see Fig. 6). Phase responses are the upper curves and amplitude responses the lower ones. The primary use of this analysis is to determine the stable and unstable conditions of the practical regulator (Nyquist's criterion).

voltage source *Esensor* expressed as a function of the current flowing across itself:

$$V(\text{out}) = i(V_{\text{probemes}}) \times R[V(\text{in})] \tag{4}$$

where $i(V_{\text{probemes}})$ is measured by the zero-voltage generator V_{probemes} in series with *Esensor* and where $R[T]$ is the non-linear expression of the thermistor resistance versus the temperature T here equal to the sensor-node voltage. In the same way the reference resistor value R_{set} is set to $R[T_{\text{set}}]$, T_{set} being the reference temperature 353 K (80 °C) of the feedback system.

At the output of the electronic function of the thermal regulator the electrical power dissipated by heaters is converted into a thermal flux. This is the right end of the block in Fig. 6 where the power conversion (here the heaters are the resistor *Rheater* and the transistor *X1*) is analytically performed by the voltage-controlled current source *Gheater* and the extra voltage-to-current converter which matches it to 1/8 of the structure. Then simulation possibilities lead to a rather exhaustive analysis. In addition to the steady state analysis versus the ambient temperature (the results of which could be displayed on the schematic), it is possible to get realistic information about the system stability as well as its transient behaviour. As an example, Fig. 7 illustrates results of a "DC analysis" that is to say a time-invariant analysis. As expected one can notice that nodes close to the quartz oven are less sensitive to the external temperature than those which are more far away from it . Thus the static thermal gain and the operating range of the thermal regulation can easily be calculated. In the present case the regulator turns off at a little bit more than 323 K (50 °C). This is obviously the consequence of the existence of the internal power dissipated by the electronic components. This operating limit could be estimated by taking into account the overall thermal resistance between the heart of the device and the external case when the reference temperature is set to 353 K (80 °C) (because of the quartz turn-over temperature).

Fig. 8 shows an example of the amplitude and phase response of the thermal regulator to an external temperature disturbance for various adjustments of the regulator integration time constant. The simulated disturbance is a sine voltage $V(T_{\text{amb}})$ equivalent to a sine temperature deviation in the electrical analogy. It is the input stimulus for the basic analysis of the frequency response of the servo system whose primary requirement is to be stable. Then the Nyquist's stability criterion can be applied to this closed loop system containing a mixture of thermal and electronic transfer functions. The detailed analysis of these curves is beyond our paper's subject but one can easily guess that the relative location of the sensor (see "*probe1*" in Fig. 4) versus the monitored power (see "*ovenpower*" and "μ *power*") is also greatly as important as the integration time constant in the stability conditions. As an illustration of the simulation capabilities in transient analysis, Fig. 9 shows the behaviour of monitored

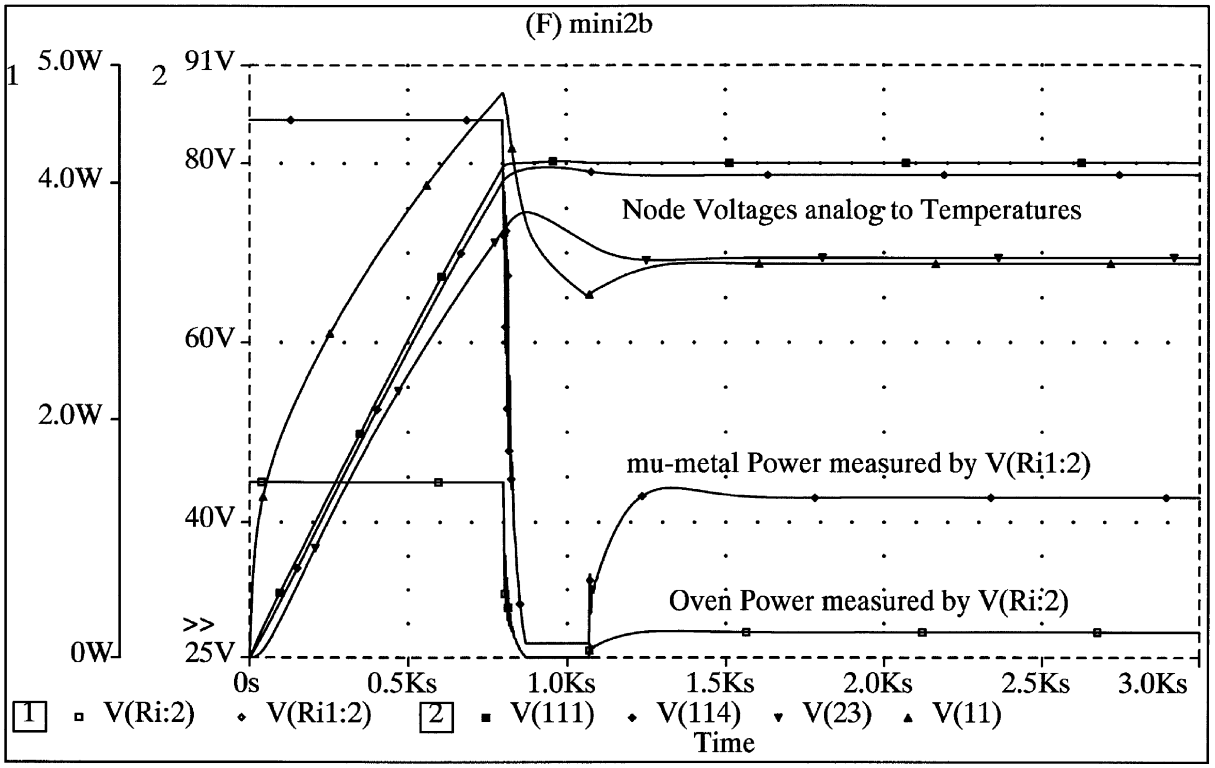

Fig. 9. Transient analysis results (warm-up).The Y axis #1 is the power axis, the Y axis #2 is the voltage axis where node voltages are still equivalent to node temperatures. At $Time = 0$ the overall structure is at the ambient temperature (here 25 °C or V!) when the electronic supply is turned on. The thermal regulator first saturates (the oven power has been limited to 1.5 W and the μ metal power to 4.5 W) before working in a linear mode and reaching its steady state (the monitoring powers are then equal to those given in Fig. 7, at $Text = 25\,°C$ in this case). As long as the thermistor temperature has not reached the reference temperature (353 K = 80 °C , here 80 V in the electrical analogy!) the system is working in such a transient period. Here are shown the temperature behaviours of the nodes already selected in Fig. 7.

powers when the device is turned on (the total available power must often be limited) and gives the warm-up time (here at the ambient temperature $T_{amb} = 298\ K = 25\,°C$). In this example local temperatures may reach inappropriate values (see $V(11)$ in Fig. 9) since the controlled power is shared between three areas of the structure. All these illustrations show how convenient the simulation is to quickly anticipate and correct any potential flaws of the thermal regulator design!

The above results just concern the thermal point of view but one cannot forget that the electronic functions can obviously be simulated (this is the major use of this Electronic Design Aided software!). For space applications severe part-stress rules exist for instance and simulations give the opportunity to guarantee them.

5. Conclusion

As mentioned, the analysed structure is manually discretized. this is a limitation of this methodology. Otherwise it is just a matter of a trade off between the accuracy related to the mesh thinness and the computation time.

We are using a standard of the electronic simulation ("SPICE"). This widespread tool in electronic circuit simulation is easy to use and has been thoroughly debugged an improved for years. Therefore our approach yields a very fast and reliable model in the first stage of a thermal design for any kind of oscillator. For space applications the overall design of an ultra stable oscillator also needs mechanical analysis usually performed with a finite element software. Thus a finite element thermal analysis can also be derived from the mesh of elements built for mechanical analysis and compared to the electro-thermal "SPICE" simulation for mutual validation.

The advantages of the methodology described in this paper come from its multiple capabilities which are listed here.

- The feedback control system stability and its efficiency over a large external temperature range, versus the sensor and power element positioning. The behaviour of the open-loop and closed-loop transfer functions in a linear process and the effect of various disturbances (external temperature, supply voltage, component limitations ...) including non-linear effects can be easily performed.
- The effects of various thermal boundary conditions (air, vacuum) according to the material properties (thermal conductivity, emissivity ...).
- Component deratings and part stress.

Thereby, since many years this methodology is constantly refined and systematically exploited in all our temperature regulation achievements. These simulations are also very fruitful in the experimental adjustment operations.

Acknowledgement

The authors wish to thank Prof. E. Bigler for his helpful comments and Ph. Guillemot for trusting us.

References

[1] R.J. Besson, M. Mourey, S. Galliou, F. Marionnet, F. Gonzalez, Ph. Guillemot, R. Tjoelker, W. Diener, A. Kirk, 10 MHz hyperstable quartz oscillators, in: Proceedings of the Joint meeting of the 13th European Frequency and Time Forum and 1999 IEEE International Frequency Control Symposium, April, 1999, pp. 326–330.

[2] A. Ballato, J.R. Vig, Static and dynamic frequency-temperature behavior of singly and doubly rotated, oven-controlled quartz resonators, in: Proceedings of the 32nd Annual Frequency Control Symposium, 1978, pp. 180–188.

[3] G. Théobald, G. Marianneau, R. Pretot, J.J. Gagnepain, Dynamic thermal behavior of quartz resonator, in: Proceedings of the 33rd Annual Frequency Control Symposium, 1979, pp. 239–246.

[4] R.J. Besson, Résonateur à quartz à électrodes non adhérentes au cristal, French Patent 76.010.35/76.122.89.

[5] S. Galliou, Thermal behavior simulation of quartz resonators in an oven environment, IEEE Trans. Ultrasonics Ferroelectrics Frequency Control 42 (5) (1995) 832–839.

[6] H. Vinke, C.J.M. Lasance, Compact models for accurate thermal characterization of electronic parts, IEEE Trans. Components Packaging Manufacturing Technology A 20 (1997) 411–419.

[7] C.J.M. Lasance, H.I. Rosten, J.D. Parry, The world of thermal characterization according to DELPHI, IEEE Trans. Components Packaging Manufacturing Technology A 20 (1997) 392–398.

[8] C. Harlander, R. Sabelka, R. Minixhofer, S. Selberherr, Three-dimensional transient electro-thermal simulation, in: Proceeding of the 5th International Workshop Thermal Investigations of ICs and Systems, Therminic Roma, Italy, 1999, pp. 169–172.